Journal of the Brazilian Society of Mechanical Sciences and Engineering (2018) 40:259
https://doi.org/10.1007/s40430-018-1186-5

TECHNICAL PAPER

Modelling and multi-objective optimization of surface roughness and kerf taper angle in abrasive water jet machining of steel

Parikshit A. Dumbhare[1] · Shikha Dubey[1] · Yogesh V. Deshpande[1] · Atul B. Andhare[2] · Purushottam S. Barve[3]

Received: 18 January 2018 / Accepted: 18 April 2018 / Published online: 24 April 2018
© The Brazilian Society of Mechanical Sciences and Engineering 2018

Abstract

Abrasive water jet machining (AWJM) is a popular method used for cutting purposes. It uses a thin jet of ultra-high pressure water and abrasive slurry to cut the material and the cutting is mainly by erosion. The purpose of this paper is to investigate the effect of AWJM parameters on the cutting of mild steel and to optimize the process parameters. The process parameters considered for investigation are traverse speed, abrasive flow rate and standoff distance. The subsequent response parameters that have been determined are surface roughness and kerf taper angle. Taguchi L_9 orthogonal array has been used to design the experiments. ANOVA is used to decide the influencing process parameters. 3D surface plots are presented for interaction effects of input process parameters. The study revealed that traverse speed is the prime factor influencing surface roughness and kerf taper angle followed by stand-off distance and abrasive flow rate. Response models are verified on the basis of estimation capability. Later on, multi-objective optimization using response surface methodology has been used for minimizing surface roughness and kerf taper angle which further resulted in composite desirability of 0.9497. The optimum values of abrasive flow rate, standoff distance and traverse speed are found to be 420 g/min, 3 mm and 85 mm/min, respectively. To validate the results, confirmation test is performed using optimum cutting parameters. It showed 9.17 and 8.57% error for surface roughness and kerf taper angle.

Keywords Abrasive water jet machining · Response surface methodology · Surface roughness · Kerf taper angle · Multi-objective optimization

1 Introduction

Abrasive water-jet machining (AWJM) process has a rich history, which dates back to the time of hydraulic gold mining in California, during the 1800s [1]. AWJM is the method of removal of material from a workpiece due to the erosive exploit of fine-grained abrasive particles colliding with it at high velocity. The particles pass through a nozzle with dense carrier gas, generally air, to reach the high velocity. The primary mechanism of the process is material erosion by the means of water jet impingement, such that the force and change in momentum of the abrasive material erodes the work material [1–3]. Here, each hard abrasive particle acts like a single point cutting tool. It is mostly used in machining of soft metals and hard materials such as ceramics, glass, metals, and composite materials [4]. Abrasive water-jet machining (AWJM) technology has wide usage in automobile and aerospace industries due to various advantages such as no generation of fumes, capacity to generate contours, no thermal distortion, good surface quality, high machining versatility, negligible burrs, etc. [5].

The accomplishment of machining process depends on the appropriate selection of cutting conditions based on cost and quality factors. A quality measurement of a product and a factor that significantly affects the manufacturing cost is surface roughness [6]. Since, high quality of

Technical Editor: Márcio Bacci da Silva.

✉ Yogesh V. Deshpande
deshpandeyv@rknec.edu; deshpande_yv@yahoo.co.in

Purushottam S. Barve
purubarve5@yahoo.co.in

1 Department of Industrial Engineering, Shri Ramdeobaba College of Engineering and Management, Nagpur 440013, India

2 Department of Mechanical Engineering, Visvesvaraya National Institute of Technology, Nagpur, India

3 Department of Mechanical Engineering, Yeshwantrao Chavan College of Engineering, Nagpur, India

surface finish is an intensified demand in various manufacturing fields like aerospace, automobile, robotics, etc. [7, 8], it is an important performance indicator for machining. Kerf geometry is another important attribute in abrasive water jet cutting. Kerf geometry is distinguished by surface topography such as waviness and roughness along with kerf width and taper angle [9]. It has an extensive access and as the jet cuts into the material, its width decreases and kerf is formed. Variation per millimeter of penetration as much as half of kerf width can be defined as kerf taper. Kerf tapers are developed as the jet loses its power, it pierces from the top surface to bottom [10]. The research works focused on AWJM is discussed in the following paragraphs.

The effect of water pressure, traverse speed and standoff distance on surface roughness in machining of mild steel by AWJM have been studied by Rao et al. [11]. They used Taguchi's method and analysis of variance (ANOVA) for examining the input process parameters along with signal to noise ratio (SN ratio) to optimize the considered parameters. They concluded that the transverse speed and water pressure are the major influencing and standoff distance is sub influencing parameter on surface roughness. The effects of traverse speed, abrasive mass flow rate and material thickness on surface roughness while machining aluminum with abrasive water jet have been reported by Begic-Hajdarevic et al. [12]. They evaluated that the surface roughness at the base of the cut is greatly influenced by traverse speed. Mutavgjic et al. [2] performed machining of stainless steel and aluminum by water jet machining. They studied the effect of stand-off distance, abrasive flow rate, transverse rate and water pressure. They concluded that surface roughness is directly proportional to traverse speed. Aultrin1 et al. [13] investigated the effect of process parameters such as pressure, abrasive flow rate, orifice diameter, focusing nozzle diameter and standoff distance in machining of aluminum alloy. They developed second-order polynomial model for prediction of material removal rate (MRR) and surface roughness using RSM. Santhankumar et al. [14] reported the effect of water pressure, abrasive grain size, nozzle–workpiece standoff, abrasive flow rate and jet traverse speed on the surface roughness and kerf angle using Taguchi's method. A combined method of grey-based response surface methodology was used for finding the optimal level of AWJM parameters. Nair and Kumanan [15] performed machining of nickel alloy and studied multiple responses using input parameters such as water jet pressure, abrasive mass flow rate and standoff distance. Significance of input parameters on multi-response were studied. It was found that water jet pressure is most significant parameter followed by mass flow rate on kerf taper angle and surface roughness. Ahmet et al. [16] also performed machining of difficult to cut titanium alloy. They examined the effect of traverse speed on machined surface characteristics and found that traverse speed is the most significant parameter. They also reported that by increasing traverse speed, the kerf taper ratio and surface roughness increases. Babu et al. [17] focused on process parameters in abrasive water jet machining with the objective of reducing surface roughness in Brass-360. The input factors were pump pressure, abrasive flow rate, standoff distance and feed rate. Pump pressure was found to be the most influencing factor on surface roughness. RSM modelling and optimization technique was used to choose the prime factors that reduced the surface roughness. Kumar et al. [18] formulated the relation between process parameters and response parameters using RSM in machining of Nickel alloy. Abrasive flow rate, water pressure, stand-off distance and traverse speed were the input parameters considered to predict surface roughness. It was observed that traverse speed and abrasive flow rate has a most significant effect on surface roughness followed by stand-off distance. However, water pressure was found to be the most insignificant parameter. Azmir et al. [19] carried out experimentation on Kevlar- phenolic composite by implementing Taguchi method. They analyzed the effect of input parameters (abrasive-mass flow rate, pressure, traverse rate and standoff distance) on surface roughness and kerf taper ratio. The traverse rate is a most significant factor on surface roughness compared to standoff distance and abrasive mass flow. Armağan et al. [20] performed Taguchi experimental design and ANOVA analysis in jet machining of glass–vinyl ester composite. They found that stand-off distance proved to be the most effective process parameter for kerf width. This was due to the divergence effect of the water jet. However, the top kerf width was a bit affected by the traverse speed as less number of particles were hitting the kerf edge. Jagadish et al. [21] developed a RSM-based optimization design for optimization of AWJM parameters on machining of green composites. The process parameters were pressure within the pumping system, stand-off distance, and nozzle speed whereas response parameters were surface roughness and process time. The trials were executed based on the Box-Behnken design and best parameters were selected using multi-response optimization. Khan and Hague [22] evaluated the effect of different abrasive particles in machining of glass using abrasive water jet. They reported that an increase in standoff distance widens the water jet and results in increase of kerf taper. The jet depth increases with increases in hardness of abrasives. The estimation of the kerf formation over ceramic plate is reported by Hocheng and Chang [23]. It is established that a critical grouping of hydraulic pressure, abrasive flow rate and traverse speed is necessary during cutting of ceramics. Adequate supply of hydraulic energy, fine mesh abrasives at reasonable speed

gives smooth kerf surface. It is concluded that the kerf width enhances with rising pressure, traverse speed, abrasive flow rate and abrasive size. Moreover, the taper ratio increases with a boost in traverse speed. Gupta et al. [24] investigated machining of marble for minimization of kerf taper angle and kerf width using Taguchi's method in the abrasive water jet. They used parameters as water pressure, nozzle traverse speed and abrasive flow rate and concluded that the nozzle traverse speed is the most influencing factor on responses.

It is observed that the researchers have discussed the effect of AWJM cutting parameters on various responses. The modelling and optimization techniques are generally preferred to predict the response and to evaluate the optimum process parameters. On the basis of the literature, it can be observed that very less amount of work is carried out on modelling and optimization of input parameters of AWJM in machining of popularly used material like mild steel. Therefore, in this paper, an attempt has been made using three process input parameters to examine the effect of machining parameters on mild steel in terms of surface roughness and kerf taper angle. Response surface methodology (RSM) is used for modelling and to investigate the interaction effects on response parameters. The multi-objective optimization technique is also used to obtain the optimal values for minimization of response parameters.

2 Experimentation

2.1 Work material and experimental setup

In the present work, a mild steel sheet of size 1000 mm × 800 mm with 6 mm thickness is used for cutting 30 mm × 50 mm plates during experimentation. The setup consist of a TOPS (Model: SJA T300) AWJM unit as shown in Fig. 1. The unit has a direct drive pump and active cutting head. It has a maximum load capacity of 1200 kg/m^2 and a linear accuracy of ±0.05 mm. The cutting head consists of a mixing chamber for sand and water jet along with sapphire jewel with an orifice diameter of 0.1 mm and a carbide nozzle with a lifespan of 100 h. Abrasive garnet (SiO_2) with mesh size of #80 is used. The unit is loaded with an inbuilt software TOPSMASTER where input parameters are entered. The cutting area is 3.05 m long and 1.55 m wide. The cutting head can move in the Z-axis over a distance of 200 mm. It has a maximum traverse speed of 15,000 mm/min.

2.2 Design of experiment

The design of experimentation (DOE) is carried out using Taguchi's L_9 orthogonal array. DOE using Taguchi method is simple and easy to imply. It swiftly confines the field of research work in a minimum number of experimentation [25, 26]. In this experimentation, three input factors: traverse speed, standoff distance and abrasive flow rate are considered. Surface roughness (R_a) and kerf taper angle (θ) are selected as responses. In Taguchi's approach, selection of the appropriate orthogonal array depends on the following three factors: (1) number of input and response factors along with the interactions that are of key importance. (2) Number of levels of data for input factors. (3) Desired resolution of experiment and the limitations placed on the cost and its performance [27]. Table 1 shows the three input factors with 3-levels which are selected according to the literature [28].

Design matrix for experimentation is generated using Taguchi approach in MINITAB 17 software and presented

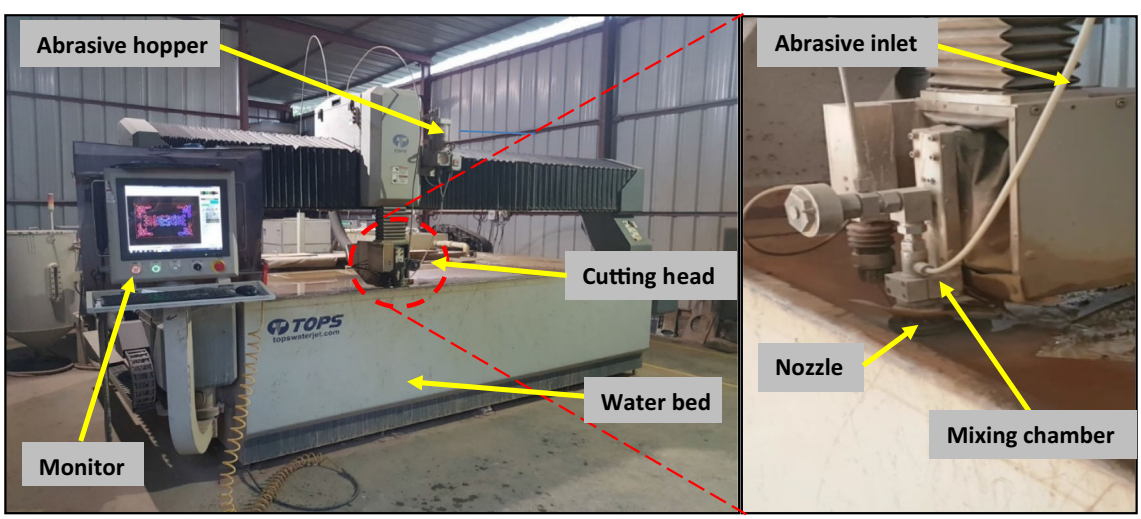

Fig. 1 Experimental setup of AWJM (left) and cutting head (right)

Table 1 Levels of input factors

Process parameters	Level 1 (− 1)	Level 2 (0)	Level 3 (+1)
Abrasive flow rate, A_f (g/min)	390	420	450
Stand-off distance, S_d (mm)	3	5	7
Traverse speed, T_v (mm/min)	85	241	567

Table 2 Design matrix and measured responses

Run order	Abrasive flow rate, A_f (g/min)	Standoff distance, S_d (mm)	Traverse speed, T_v (mm/min)	Surface roughness, R_a (μm)	Kerf taper angle, θ (degree)
1	390	3	85	2.0	1.43
2	390	5	241	4.2	1.90
3	390	7	567	8.4	3.15
4	420	3	241	3.2	1.67
5	420	5	567	6.3	2.88
6	420	7	85	2.8	1.49
7	450	3	567	5.3	2.16
8	450	5	85	2.6	1.19
9	450	7	241	3.5	2.08

in Table 2. After experimentation, the roughness of the machined surface is measured using portable surface roughness tester (Model: Surftest SJ-410, Make: Mitutoyo) as shown in Fig. 2. The average of four measurements of surface roughness (R_a) is measured. Absolute digimatic caliper (Make: Mitutoyo) is used for measurement of upper and lower kerf width. The measured response is considered for kerf taper angle. Inclination of kerf wall is measured for obtaining the kerf taper angle at kerf edge as shown in Fig. 3. Kerf taper angle (θ) is calculated using Eq. 1 on the thickness of workpiece [29].

$$\theta = \tan^{-1}\left(\frac{W_t - W_d}{2t}\right), \quad (1)$$

where θ is kerf taper angle; W_t is upper kerf width; W_d is lower kerf width and t is the thickness of the machined workpiece. The measured responses are tabulated in Table 2 for further analysis.

3 Result and discussion

3.1 Modeling using RSM

Response surface methodology (RSM) is generally considered in the framework of the design of experiment. It is a statistical technique for modelling and examining of difficulties in which a response of interest is affected by various variables. With aim of finding the correlation between the response and variables is its primary objective [30–32]. Determining a proper estimation for the accurate functional relationship between the response variable (y) and a set of independent variables is presented in Eq. 2.

$$y = P_0 + \sum_{i=1}^{k} P_i X_i + \sum_{i=1}^{k} P_{ii} X_i^2 + \sum \sum_{i<j} P_{ij} X_i X_j + \varepsilon, \quad (2)$$

Fig. 2 Surface roughness tester

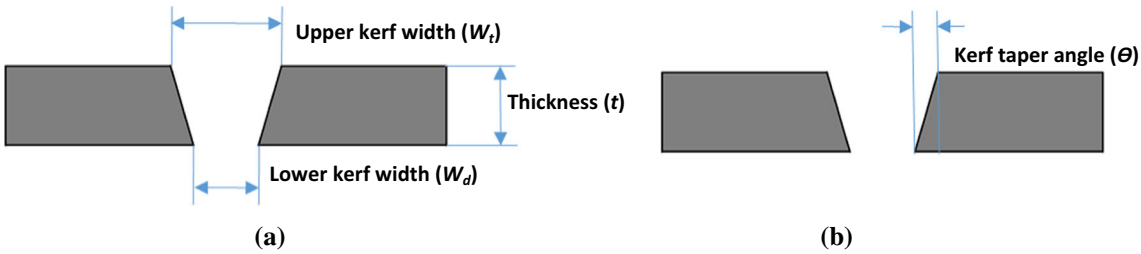

Fig. 3 Schematic of kerf profile

where P are the coefficients that are calculated using least square method and RSM is executed by means of fitted surface. When estimated surface is an acceptable estimation of the true response function, the outcomes will be nearly equivalent to examination of the actual system. With the generated data, regression models are estimated using RSM to predict the values of output parameter. The predicted values are thus useful for optimizing the response parameters by having a thorough understanding of the significant parameters. Using this technique ensures that the process and the experimentation are always within control [33]. The statistical analysis showing the effect of input process parameters on responses using ANOVA is discussed in subsequent section.

3.2 Statistical analysis of parameters for surface roughness

Analysis of variance (ANOVA) is a computational method that helps to evaluate the comparative influences of each control parameter. It offers vision into the main effects, as well as interaction effects of factors. It uses a mathematical method recognized as the sum of squares to significantly analyze the variation of the control parameter.

The ANOVA study is performed to examine the statistical analysis of input parameters on output parameters (surface roughness and kerf taper angle). The significance of input parameters is investigated using of F test, p value based on the confidence level of 95% ($p < 0.05$) and determination of coefficient (R^2). To remove the insignificant effect of parameters, the stepwise regression analysis is performed. A second-order regression equation for surface roughness is presented in Eq. 3. Table 3 shows ANOVA for surface roughness.

$$R_a = -19.13 + 0.04837A_f + 5.057S_d + 0.001308T_v - 0.04167S_d \times S_d - 0.011069A_f \times S_d + 0.001203S_d \times T_v (R^2 = 99.93\%)\left(R^2_{adj} = 98.72\%\right). \quad (3)$$

The regression model (Eq. 3) indicates high F value of 2049.84 and low p value ($p < 0.05$) which merely has 0.01% chance that the value might happen due to noise resulted from Table 3. The experimental data (Table 2) is used in Eq. 3 to examine the error among experimental and predicted values. Mean absolute error (MSE) is calculated as 0.5% for surface roughness. Similarly, R^2 and R^2_{adj} values are 99.93 and 98.72%, respectively, which indicates good correlation among experimental and predicted values.

Figure 4 shows the residual plot for R_a consisting of normal probability plot, residual verses fits, histogram for residuals and residuals versus experimental values. It is seen from Fig. 4a that the residuals have close fit to a line in normal probability graph, which shows that the data is normally distributed [34]. It means that for R_a there is a good relation between measured and estimated values. Figure 4b, residual verses fits displays slightest deviation within residuals and estimated values. Residual information is shown in the histogram in Fig. 4c. Figure 4d indicates the values of residuals versus experimental data which is spread above and below zero line. It is established from the whole inspection of residual and probability graphs that the obtained model for R_a is well proficient for precise prediction.

The parametric examination in terms of studying the effects of abrasive flow rate (A_f), stand-off distance (S_d), traverse speed (T_v) on surface roughness (R_a) are presented in main effect plots shown in Fig. 5. The main effect plots show the means for each group within a categorical variable. In case of abrasive flow rate, as abrasive flow rate increases the surface roughness decreases. It can be seen from Fig. 5a, that higher surface roughness is attained at low value of flow rate while the lower roughness are obtained by high abrasive flow rate. Therefore, it is marked that increase in flow rate up to certain stage causes a smoothening result on the surface irregularities of machined surfaces [35]. In case of stand-off distance, the surface roughness is remarkably greater when the stand-off distances increased from 3 to 7 mm shown in Fig. 5b. This is for the reason that greater stand-off distance causes the divergence of jet before impingement. This results in reduced kinetic energy density of the jet at impingement resulting in rougher surface. This jet divergence leads to low density of abrasive particles [21, 36]. Hence, it is

Table 3 ANOVA for surface roughness

Source	Sum of squares	*DF*	Mean square	*F* value	*p* value
Regression model	34.07	6	5.67	2049.84	< 0.0001
A_f	0.13	1	0.13	50.11	0.019
S_d	3.40	1	3.40	1229.43	0.001
T_v	10.29	1	10.29	3716.69	< 0.0001
$S_d \times S_d$	0.05	1	20.05	20.05	0.046
$A_f \times S_d$	0.89	1	321.33	321.33	0.003
$S_d \times T_v$	0.70	1	255.28	255.28	0.004
Error	0.0055	2	0.0028		
Total	34.0822	8			
R^2				99.93%	
R^2_{adj}				98.72%	

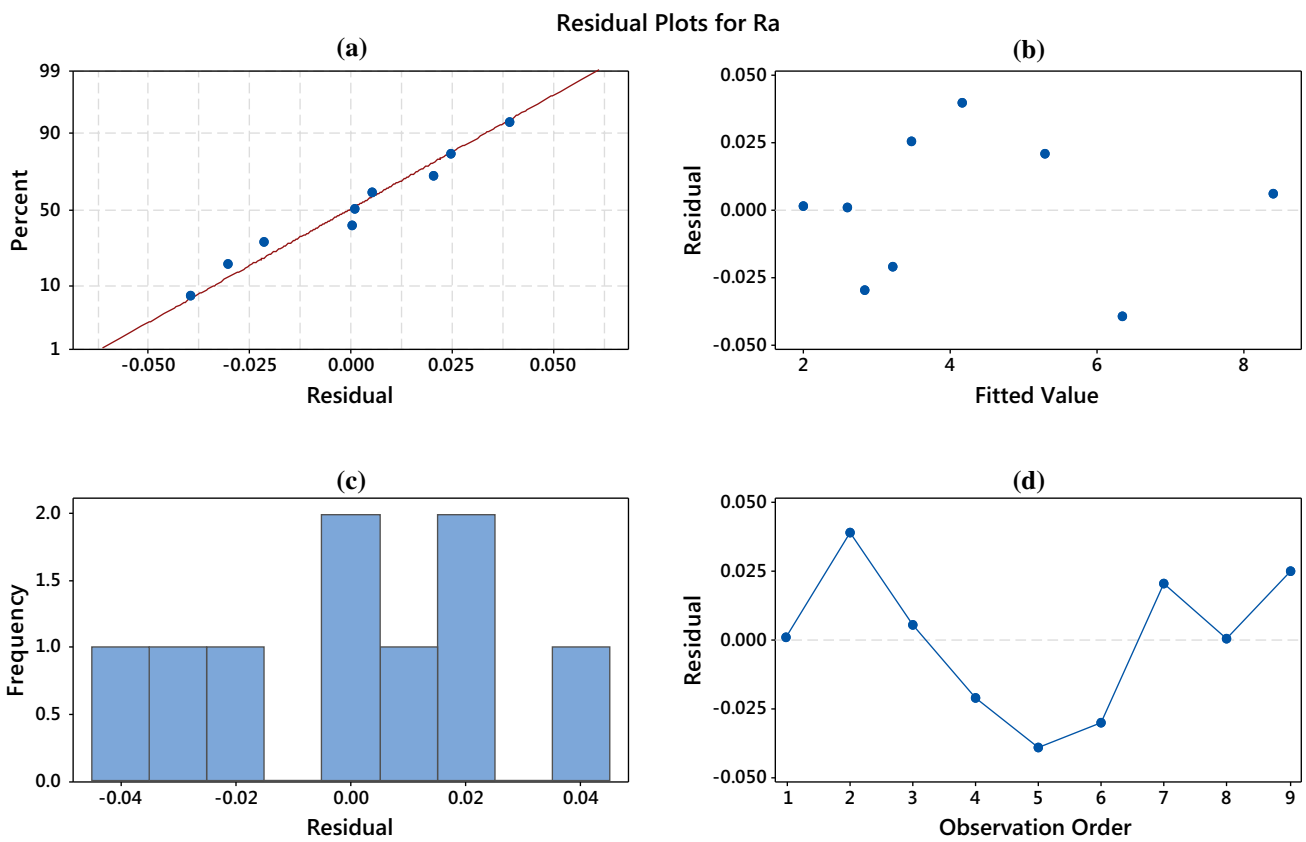

Fig. 4 Residual plot for surface roughness (R_a)

anticipated that a lower stand-off distance can yield better-machined surface. In case of traverse speed as shown in Fig. 5c, increase in speed cause fewer number of particles available that passes through a unit area. Thus, lesser amount of impacts and cutting edges will be available per unit area that fallouts in rougher surfaces. Therefore, increasing traverse speed increases the surface roughness [36].

Figure 6 indicates the dual effect of two parameters which are expressed in interaction using 3D surface plots. In Fig. 6a the standoff distance is shown versus abrasive flow rate by keeping traverse speed at mid-value of 241 mm/min and their effect on surface roughness can be learned. For lower standoff distance and higher abrasive flow rate, surface roughness decreases. Similarly, at higher standoff distance and lower abrasive flow rate, surface roughness increases. This is due to the reason that as standoff distance increases, the driving force of particles colliding the workpiece reduces, resulting in the development of uneven peaks on the machined surface. In

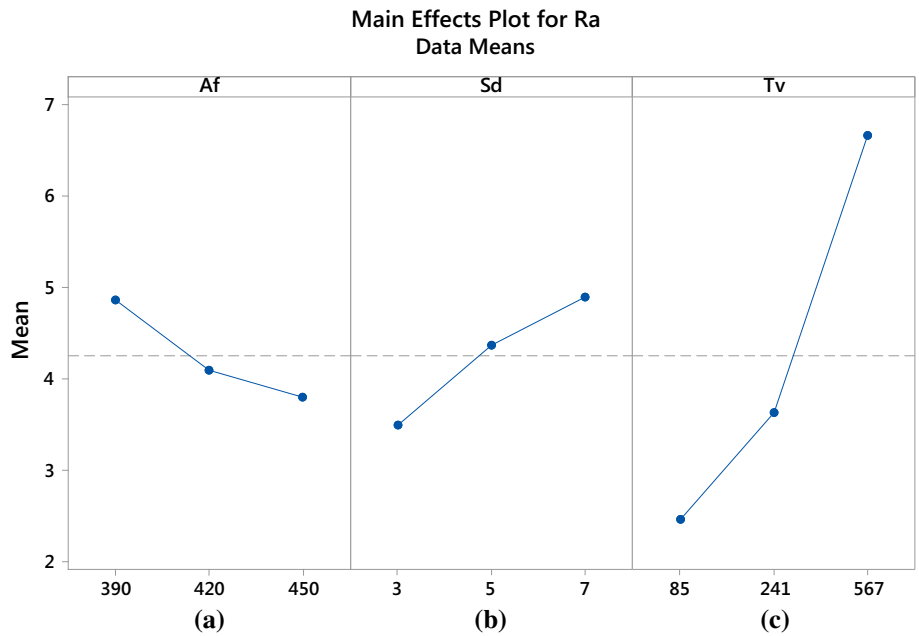

Fig. 5 Main effect plot for R_a

Fig. 6b the 3D response surface corresponds to the interaction of abrasive flow rate and traverse speed at a constant standoff distance of 5 mm. Here, for the high value of traverse speed and low value of abrasive flow rate, increase in surface roughness value is observed and vice versa. This is because low particles collide on the surface with less amount of time for cutting of the workpiece. Figure 6c shows the combination of standoff distance and traverse speed at constant abrasive flow rate of 420 g/min, high surface roughness is observed when the value of standoff distance and traverse speed is high. Similarly, lower surface roughness is observed at minimum standoff distance and less traverse speed. This occurs because it allows the particles of the jet to bombard with greater force and allowing sufficient amount of time for cutting.

3.3 Statistical analysis of parameters for kerf taper angle

Similarly, in case of kerf taper angle, a second-order quadratic equation is formed by eliminating insignificant terms from the model using stepwise deletion method. Table 4 shows the significant parameters according to their F values and p values. The regression model shows F value of 1285.33 and p value of 0.001 indicating that the model is significant. Here also, merely 0.1% chance that this F value might happen due to noise. Using stepwise elimination method with 95% of confidence level ($p < 0.05$), the regression model for kerf taper is refined and shown in Eq. 4.

$$\theta = -6.02 + 0.0501A_f - 1.122S_d + 0.001755T_v - 0.000080A_f \times A_f + 0.002761A_f \times S_d + 0.000280S_d \times T_v \quad (R^2 = 99.90\%)\left(R^2_{adj} = 99.54\%\right). \tag{4}$$

Residual and probability graphs for kerf taper angle of experimental specimen are shown in Fig. 7. The graphs showed that there is normal distribution of data specifying that residuals have close fit to a line in normal probability graph. A good relation is observed between measured and estimated values of θ. These test settings are fulfilled which visibly specify that the reliability of the observations is up to the mark and follows 95% confidence interval.

The effect of the process parameters on the kerf taper angle (θ) are shown in main effect plots. As abrasive flow rate increases kerf taper angle *(θ)* reduces as shown in Fig. 8a. When the stand-off distance increases, increment in kerf taper angle *(θ)* is shown in Fig. 8b. This is because the diameter of the jet increases before bombarding on workpiece making lower kerf width smaller than upper kerf width. In Fig. 8c it can be seen that increment in traverse speed increases the kerf taper angle. This is for the reason that as the traverse speed increases the broadening of the kerf lower part by the jet decreases.

Figure 9a shows the interaction effect of abrasive flow rate and standoff distance keeping traverse speed constant at 241 mm/min. For higher abrasive flow rate and low stand-off distance the value of kerf taper angle decreases. Whereas at higher standoff distance and lower abrasive flow rate, rise in kerf taper angle is observed. This is due to the fact that as standoff distance increases and abrasive

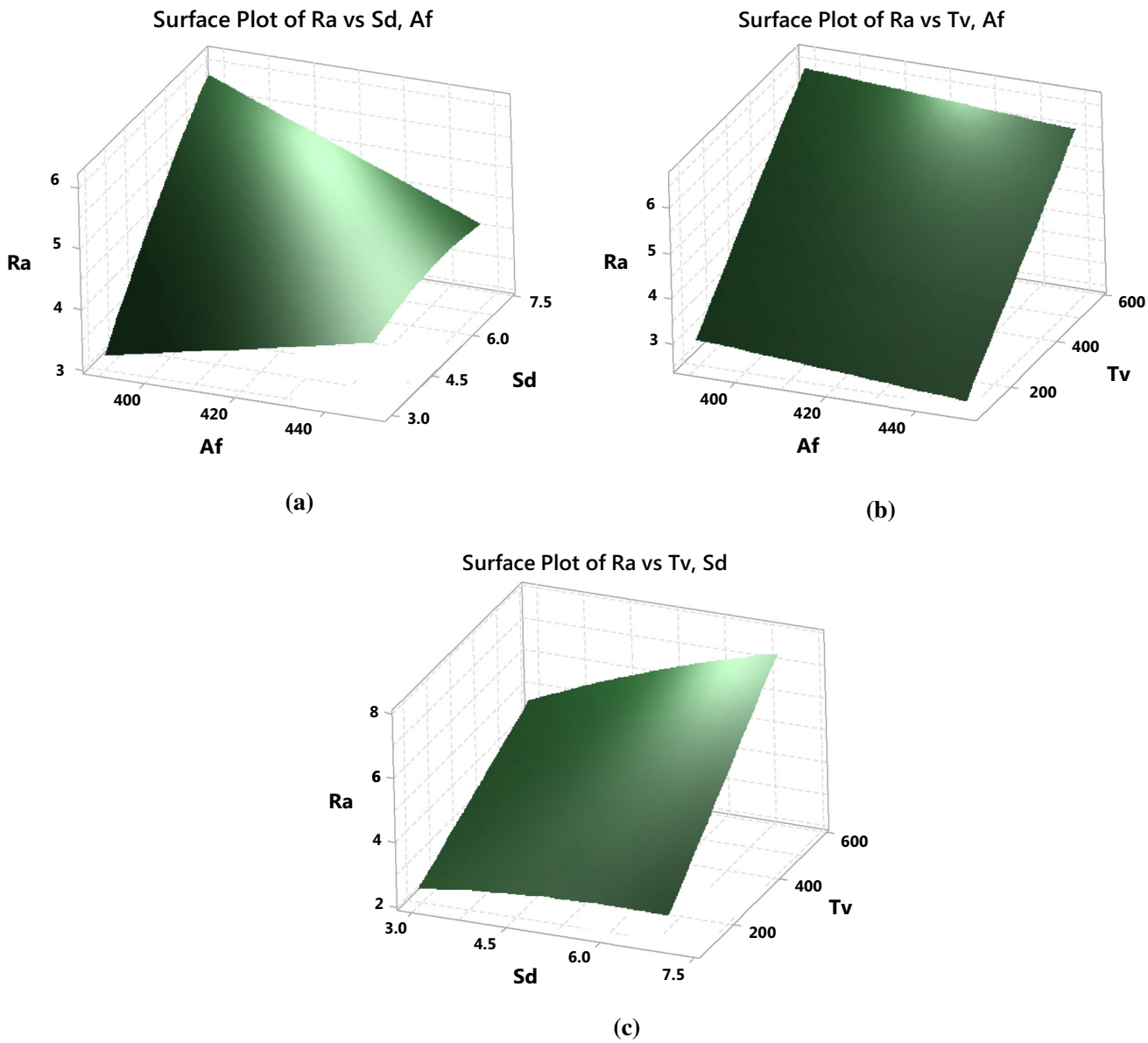

Fig. 6 3D surface plots R_a

Table 4 ANOVA for kerf taper angle (θ)

Source	Sum of squares	*DF*	Mean square	*F* value	*p* value
Regression model	3.48	6	0.581	1285.33	0.001
A_f	0.02	1	0.029	66.02	0.015
S_d	0.38	1	0.386	854.04	0.001
T_v	1.90	1	1.903	4208.74	< 0.0001
$A_f \times A_f$	0.009	1	0.009	20.68	0.045
$A_f \times S_d$	0.054	1	0.0549	121.39	0.008
$S_d \times T_v$	0.034	1	0.0345	76.39	0.013
Error	0.0009	2	0.00045		
Total	3.4886	8			
R^2				99.90%	
R^2_{adj}				99.54%	

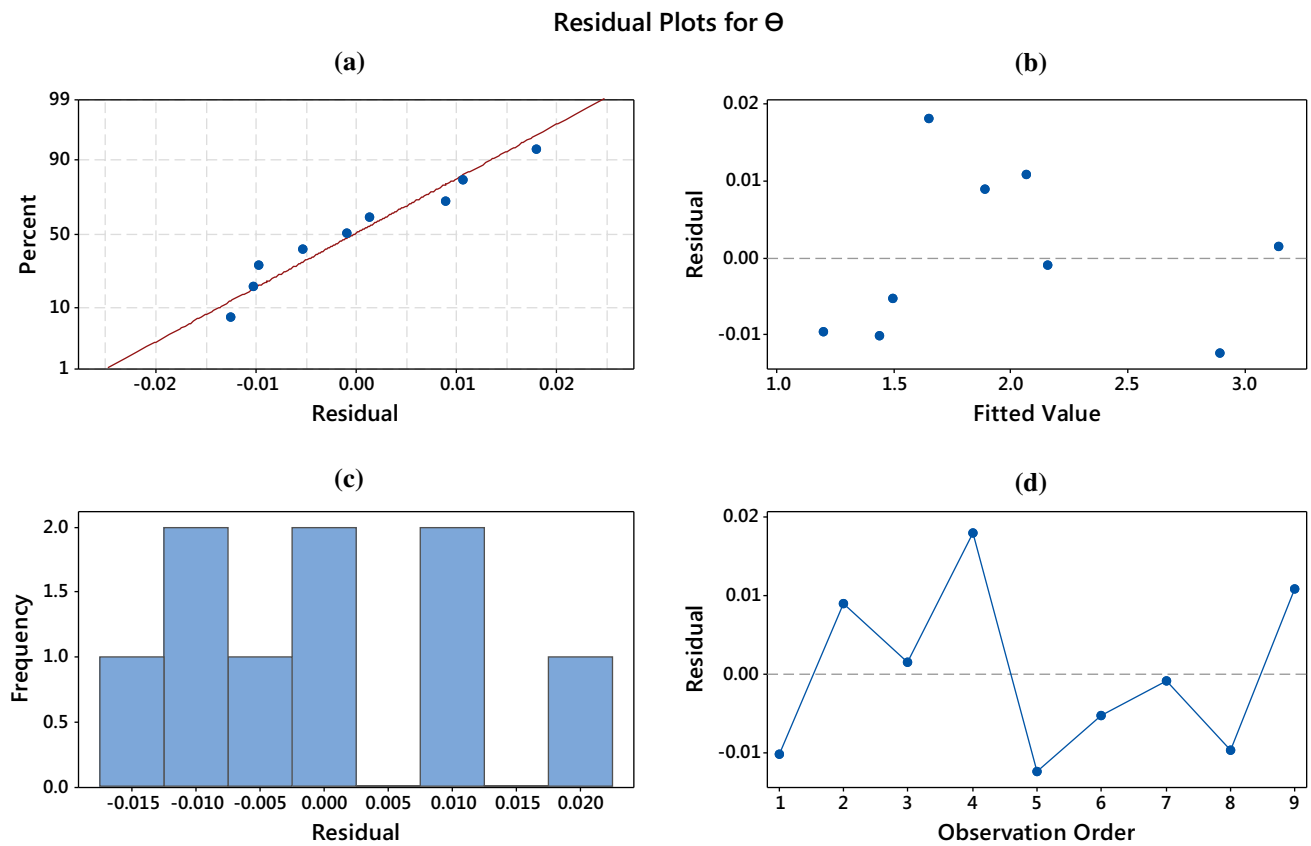

Fig. 7 Residual plot for θ

Fig. 8 Main effect plot for θ

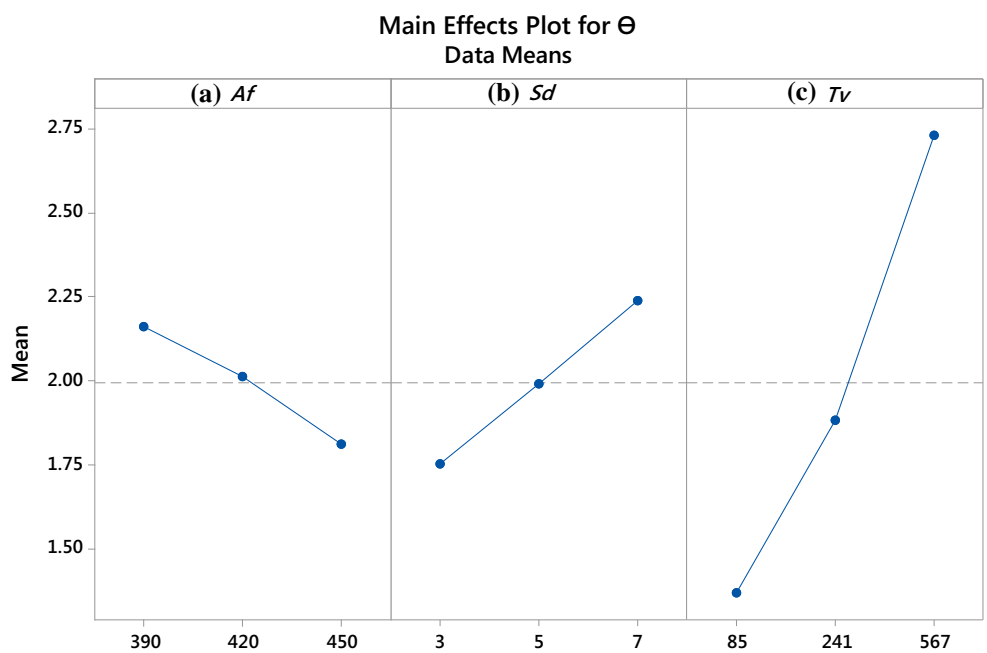

flow rate decreases, sufficient abrasive particles are not available. Hence, not allowing the jet to penetrate properly. Figure 9b indicates the interaction of abrasive flow rate and traverse speed where for greater value of traverse speed and lower value of abrasive flow rate, kerf taper angle increases. Here, standoff distance is kept perpetual at 5 mm. But, even at higher abrasive flow rate and higher traverse speed, no significant change can be observed. This

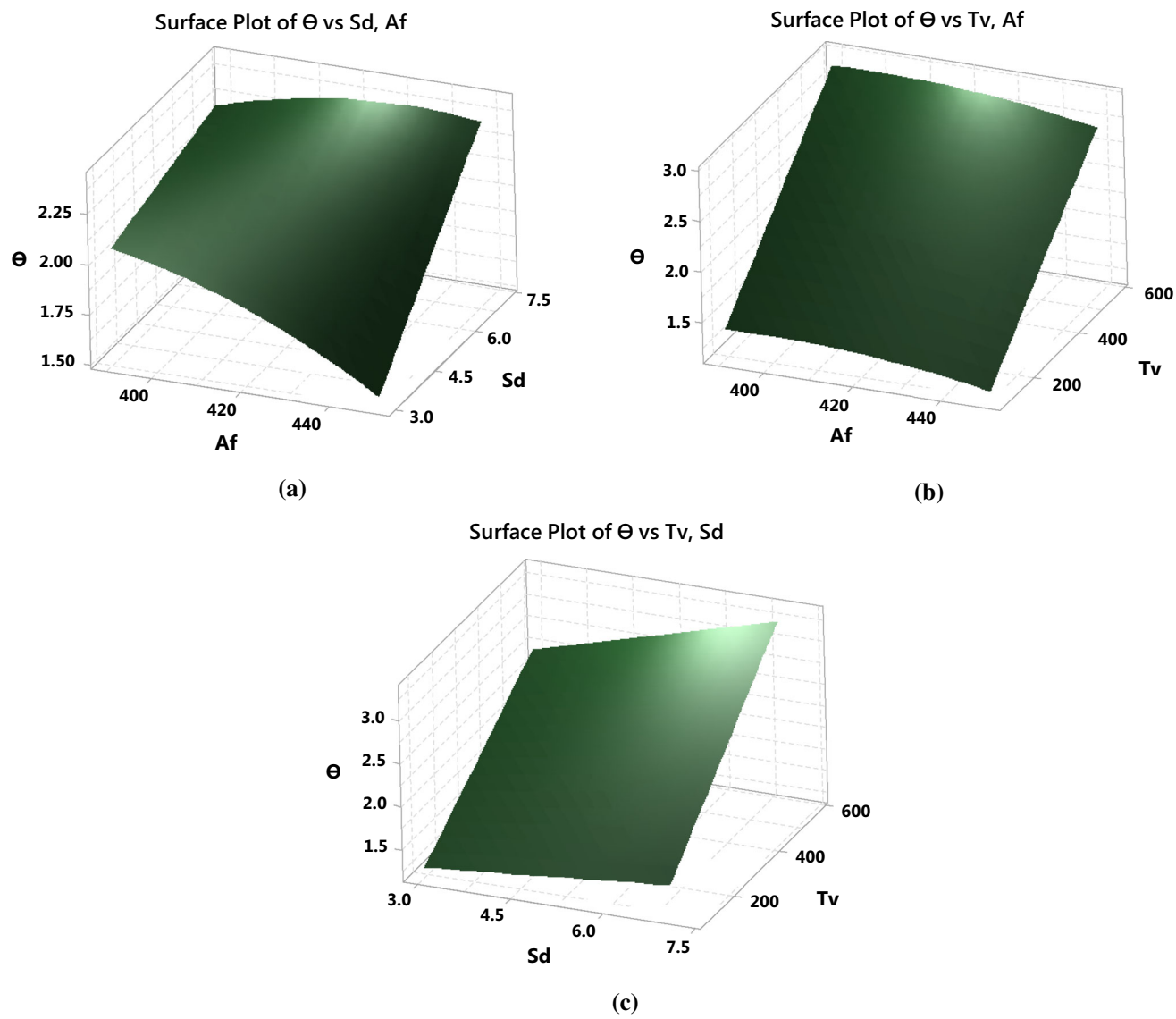

Fig. 9 3D surface plots for θ

is due to the higher effect of traverse speed on kerf taper angle than abrasive flow rate. It is observed in Fig. 9c that for increase in value of traverse speed and standoff distance there is boost in value of kerf taper angle keeping value of abrasive flow rate at 420 g/min. Similarly, low stand-off distance and low value of traverse speed results in lowest kerf taper angle. This is because low standoff distance allows abrasive particles to pierce workpiece with high kinetic energy density and low traverse speed increase the number of abrasive particles impinging the workpiece.

3.4 RSM optimization

Optimization algorithms processes are started by picking up the several point for finding of optimum parameters. Two solution types for finding the optimal values are local and global solution. From all the local solutions, the global solution is one of the finest solution which is regarded as the pre-eminent relation of input factors for achieving the optimal response. For optimization of response factors (R_a, θ) RSM desirability function is used. In desirability approach, all response values are converted into non-dimensional desirability value (d) that changes in the scale of 0–1. Response value is completely undesirable, when $d = 0$. Whereas $d = 1$ shows the acceptability of the response. Geometric mean of each single desirability (di) are measured in combination. Equation 5 shows the objective function of total desirability.

$$D = \left(\prod_{i=1}^{n} d_i^n \right)^{\frac{1}{\sum^{ri}}}. \tag{5}$$

Table 5 Constraint for optimization of AWJM machining parameters

Condition	Goal	Lower limit	Upper limit
Abrasive flow rate A_f (g/min)	In range	390	450
Standoff distance S_d (mm)	In range	3.0	7.0
Traverse speed T_v (mm/min)	In range	85	567
Surface roughness R_a (μm)	Minimize	2.0	8.4
Kerf taper angle θ (degree)	Minimize	1.19	3.15

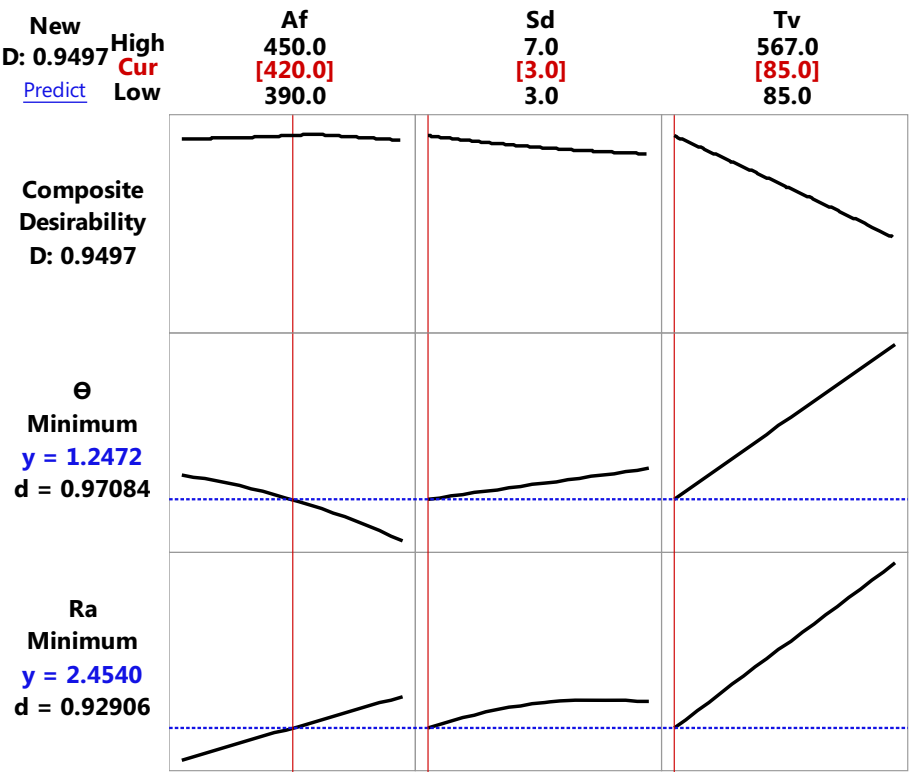

Fig. 10 Response optimization plot

D indicates the objective function of total desirability and r shows the response significance with other responses. If value of D is higher, it indicates the finest function and high desirability attaining the optimum values of response parameters [26, 34, 37].

In this research, multi-objective optimization is performed using RSM for optimizing input parameters with respect to surface roughness and kerf taper angle. The constraints used through the optimization process are summarized in Table 5. During optimization, equal weights are distributed among both responses (R_a, θ). Figure 10 shows the composite desirability of 0.9497 for optimization of responses which indicates that the solution is acceptable. Optimal process parameters obtained are abrasive flow rate (A_f) = 420 g/min, standoff distance (S_d) = 3 mm and traverse speed (T_v)- = 85 mm/min.

3.5 Validation of models

Three fresh experiments are conducted for confirmation of models Eqs. (3) and (4), with achieved optimal values of cutting parameters. The average of measured values for surface roughness and kerf taper angle are tabulated in Table 6. The accuracy of the models is analyzed on the basis percentage error. These errors are found to be 9.17 and 8.57% for surface roughness and kerf taper angle,

Table 6 Validation of process parameters

Parameters	Experimental	RSM	Error
Abrasive flow rate, A_f (g/min)	420	420	–
Standoff distance, S_d (mm)	3	3	–
Traverse speed, T_v (mm/min)	85	85	–
Surface roughness, R_a (μm)	2.70	2.45	9.17
Kerf taper angle, θ (degree)	1.36	1.24	8.57

respectively. It is possibly due to some vibrations during machining which affects the measurement techniques. Since the error is less than 10%, it is evidently proved that there is a good agreement between experimental and predicted values [38].

4 Conclusion

The current study shows the influence of the various process parameter on the corresponding response parameter while machining of mild steel. ANOVA was used to determine the importance and capability of the developed model. After confirming the capability of response models, the multi-objective optimization using RSM technique is used and following conclusions are drawn:

1. The mathematical models have been framed for surface roughness and kerf angle in terms of traverse speed, abrasive flow rate and standoff distance. ANOVA was performed to analyze the significance of input parameters. High F values and p values less than 0.05 signifies that regression models are exceptionally significant. Additionally, it resulted that traverse speed is the foremost significant factor in both responses followed by standoff distance and abrasive flow rate.
2. Mean absolute error (MSE) for surface roughness and kerf taper angle are found to be 0.53 and 0.49%, respectively. Similarly, R^2 and R^2_{adj} values for surface roughness and kerf taper angle are 99.93; 98.72 and 99.90; 99.54%, respectively. Thus, good correlation among experimental and predicted values is achieved.
3. Effects of process parameters are studied using main effect plot and 3D surface plots for both responses. It showed that increment in values of standoff distance and traverse speed leads to increase in responses. Abrasive flow rate is comparatively less significant on response parameters.
4. Multi-objective optimization using RSM is performed for minimization of surface roughness and kerf taper angle which resulted in composite desirability of 0.9497. The optimum values of abrasive flow rate, standoff distance and traverse speed are found as 420 g/min, 3 mm and 85 mm/min, respectively.
5. The confirmation test is performed using optimum cutting parameters which showed 9.17 and 8.57% of error for surface roughness and kerf taper angle. This error is within acceptable limits. It is concluded that prediction of response parameters in machining of AWJM is accurate based on estimation preciseness. Therefore, the results obtained by this study would be helpful for machining in modern manufacturing industries.

References

1. Shimizu S (2011) Tribology in water jet processes. In: New tribological ways. InTech
2. Mutavgjic V, Jurkovic Z, Franulovic M, Sekulic M (2011) Experimental investigation of surface roughness obtained by abrasive water jet machining. In: 15th International research/expert conference "trends in the development of machinery and associated technology" TMT
3. Zhao W, C-w Guo, L-j Wang, F-c Wang (2017) Study on the characteristics of pressure variation in ASJ system. J Braz Soc Mech Sci Eng 39(4):1225–1232
4. Liu H, Wang J, Kelson N, Brown R (2004) A study of abrasive waterjet characteristics by CFD simulation. J Mater Process Technol 153:488–493
5. Van Luttervelt C (1989) On the selection of manufacturing methods illustrated by an overview of separation techniques for sheet materials. CIRP Ann Manuf Technol 38(2):587–607
6. Çaydaş U, Hasçalık A (2008) A study on surface roughness in abrasive waterjet machining process using artificial neural networks and regression analysis method. J Mater Process Technol 202(1):574–582
7. Sharma VS, Dhiman S, Sehgal R, Sharma S (2008) Estimation of cutting forces and surface roughness for hard turning using neural networks. J Intell Manuf 19(4):473–483
8. Öktem H (2009) An integrated study of surface roughness for modelling and optimization of cutting parameters during end milling operation. Int J Adv Manuf Technol 43(9–10):852–861
9. Sheikh-Ahmad JY (2009) Machining of polymer composites. Springer, New York
10. Wang J, Kuriyagawa T, Huang C (2003) An experimental study to enhance the cutting performance in abrasive waterjet machining. Mach Sci Technol 7(2):191–207
11. Rao MS, Ravinder S, Kumar AS (2014) Parametric optimization of abrasive water jet machining for mild steel: Taguchi approach. Int J Curr Eng and Technol Special Issue 2:28–30
12. Begic-Hajdarevic D, Cekic A, Mehmedovic M, Djelmic A (2015) Experimental study on surface roughness in abrasive water jet cutting. Procedia Eng 100:394–399
13. Aultrin KJ, Anand MD (2014) Experimental framework and study of AWJM process for an aluminium 6061 alloy using RSM. In: Control, instrumentation, communication and computational technologies (ICCICCT), 2014 international conference on, 2014. IEEE, pp 1432–1440
14. Santhanakumar M, Adalarasan R, Rajmohan M (2015) Experimental modelling and analysis in abrasive waterjet cutting of ceramic tiles using grey-based response surface methodology. Arab J Sci Eng 40(11):3299–3311
15. Nair A, Kumanan S (2018) Optimization of size and form characteristics using multi-objective grey analysis in abrasive water jet drilling of Inconel 617. J Braz Soc Mech Sci Eng 40(3):121
16. Hascalik A, Çaydaş U, Gürün H (2007) Effect of traverse speed on abrasive waterjet machining of Ti–6Al–4 V alloy. Mater Des 28(6):1953–1957
17. Naresh Babu M, Muthukrishnan N (2014) Investigation on surface roughness in abrasive water-jet machining by the response surface method. Mater Manuf Process 29(11–12):1422–1428

18. Kumar A, Singh H, Kumar V (2017) Study the parametric effect of abrasive water jet machining on surface roughness of Inconel 718 using RSM-BBD techniques. Mater Manuf Process 1–8
19. Azmir M, Ahsan A (2009) A study of abrasive water jet machining process on glass/epoxy composite laminate. J Mater Process Technol 209(20):6168–6173
20. Armağan M, Arici AA (2017) Cutting performance of glass-vinyl ester composite by abrasive water jet. Mater Manuf Process 32(15):1715–1722
21. Bhowmik S, Ray A (2015) Prediction of surface roughness quality of green abrasive water jet machining: a soft computing approach. J Intell Manuf 1–15. https://doi.org/10.1007/s10845-015-1169-7
22. Khan AA, Haque M (2007) Performance of different abrasive materials during abrasive water jet machining of glass. J Mater Process Technol 191(1):404–407
23. Hocheng H, Chang K (1994) Material removal analysis in abrasive waterjet cutting of ceramic plates. J Mater Process Technol 40(3–4):287–304
24. Gupta V, Pandey P, Garg MP, Khanna R, Batra N (2014) Minimization of kerf taper angle and kerf width using Taguchi's method in abrasive water jet machining of marble. Procedia Mater Sci 6:140–149
25. Nair VN, Abraham B, MacKay J, Box G, Kacker RN, Lorenzen TJ, Lucas JM, Myers RH, Vining GG, Nelder JA (1992) Taguchi's parameter design: a panel discussion. Technometrics 34(2):127–161
26. Rao TB, Krishna AG, Katta RK, Krishna KR (2015) Modeling and multi-response optimization of machining performance while turning hardened steel with self-propelled rotary tool. Adv Manuf 3(1):84–95
27. Lin C (2004) Use of the Taguchi method and grey relational analysis to optimize turning operations with multiple performance characteristics. Mater Manuf Processes 19(2):209–220
28. Jain VK (2009) Advanced machining processes. Allied publishers
29. Gupta V, Garg M, Batra N, Khanna R (2013) Analysis of kerf taper angle in abrasive water jet cutting of Makrana white marble. Asian J Eng Appl Technol ISSN:35-39
30. Myers RH, Montgomery DC, Anderson-Cook CM (2016) Response surface methodology: process and product optimization using designed experiments. Wiley, New York
31. Deshpande YV, Andhare AB, Padole PM (2018) Experimental results on the performance of cryogenic treatment of tool and minimum quantity lubrication for machinability improvement in the turning of Inconel 718. J Braz Soc Mech Sci Eng 40(1):6
32. John MS, Balaji B, Vinayagam B (2017) Optimisation of internal roller burnishing process in CNC machining center using response surface methodology. J Braz Soc Mech Sci Eng 39(10):4045–4057
33. Rao KV, Murthy P (2016) Modeling and optimization of tool vibration and surface roughness in boring of steel using RSM, ANN and SVM. J Intell Manuf 1–11
34. Deshpande Y, Andhare A, Sahu NK (2017) Estimation of surface roughness using cutting parameters, force, sound, and vibration in turning of Inconel 718. J Braz Soc Mech Sci Eng 1–10
35. Sreekesh K, Govindan P (2013) Experimental Investigation and analysis of abrasive water-jet machining process. In: Proceedings of the international conference on advancements and futuristic trends in mechanical and materials engineering, pp 472-477
36. Bhowmik S, Ray A (2017) Abrasive water jet machining of composite materials. In: Advanced manufacturing technologies. Springer, pp 77–97
37. Ghodsiyeh D, Golshan A, Izman S (2014) Multi-objective process optimization of wire electrical discharge machining based on response surface methodology. J Braz Soc Mech Sci Eng 36(2):301–313
38. Deshpande Y, Andhare A, Padole P, Sahu N (2018) Application of advanced algorithms for enhancement in machining performance of Inconel 718. Indian J Eng Mater Sci (in press)